Ann. Geophys., 27, 407–416, 2009
www.ann-geophys.net/27/407/2009/

Annales Geophysicae

Spectral wave analysis at the mesopause from SCIAMACHY airglow data compared to SABER temperature spectra

M. Ern, C. Lehmann, M. Kaufmann, and M. Riese

Institute of Chemistry and Dynamics of the Geosphere (ICG-1), Forschungszentrum Juelich, Juelich, Germany

Received: 23 September 2008 – Revised: 22 December 2008 – Accepted: 2 January 2009 – Published: 23 January 2009

Abstract. Space-time spectral analysis of satellite data is an important method to derive a synoptic picture of the atmosphere from measurements sampled asynoptically by satellite instruments. In addition, it serves as a powerful tool to identify and separate different wave modes in the atmospheric data. In our work we present space-time spectral analyses of chemical heating rates derived from Scanning Imaging Absorption SpectroMeter for Atmospheric CHartographY (SCIAMACHY) hydroxyl nightglow emission measurements onboard Envisat for the years 2002–2006 at mesopause heights.

Since SCIAMACHY nightglow hydroxyl emission measurements are restricted to the ascending (nighttime) part of the satellite orbit, our analysis also includes temperature spectra derived from 15 μm CO_2 emissions measured by the Sounding of the Atmosphere using Broadband Emission Radiometry (SABER) instrument. SABER offers better temporal and spatial coverage (daytime and night-time values of temperature) and a more regular sampling grid. Therefore SABER spectra also contain information about higher frequency waves.

Comparison of SCIAMACHY and SABER results shows that SCIAMACHY, in spite of its observational restrictions, provides valuable information on most of the wave modes present in the mesopause region. The main differences between wave spectra obtained from these sensors can be attributed to the differences in their sampling patterns.

Keywords. Meteorology and atmospheric dynamics (Climatology; Waves and tides; Instruments and techniques)

Correspondence to: M. Ern
(m.ern@fz-juelich.de)

1 Introduction

Planetary scale long-period atmospheric wave modes in the mesosphere/lower thermosphere (MLT) have been reported in the literature for several decades. Most observations refer to one of the following three classes of waves. First, there are strong tidal signals at periods of 1 day or shorter. The second class of waves are equatorial waves in the latitude region of about 20° S–20° N. Mostly the observed equatorial waves are eastward propagating Kelvin waves, having periods between about 10 days and 1–2 days, but also westward propagating Rossby-gravity waves are observed in the tropics and subtropics with periods between 1.5 and 2.5 days and zonal wavenumbers 1 and 2 (Garcia et al., 2005).

The third class of waves are longer period waves mostly observed at mid- and high latitudes. For this third class of waves the observed periods can be attributed to mainly four different intervals. The first interval ranges from about 1.9 to 2.2 days, the so-called quasi-2-day wave. The second interval covers the range from about 4–7 days. Those waves are usually called 5-day waves. The third interval covers about the range 8–11 days and is called 10-day waves. And finally, the third interval ranges from about 11–22 days, commonly denoted as 16-day wave.

Quasi-2-day waves are mostly observed at westward propagating zonal wavenumber 3. This wave mode is often attributed to the (3,0) Rossby-gravity mode of the atmosphere. Quasi-2-day waves are a phenomenon of the summer hemisphere in the mesosphere but they can also penetrate across the equator in the mesopause region and above (Palo et al., 1999). The 5-day waves, 10-day waves and 16-day waves propagate westward, are usually observed at zonal wavenumber 1, and are often attributed to the (1,1), (1,2), and (1,3) Rossby normal modes of the atmosphere (e.g. Salby, 1984; Luo et al., 2002).

Many observations of longer period waves (periods longer than 1 day) at low and mid latitudes are reported from ground

Published by Copernicus Publications on behalf of the European Geosciences Union.

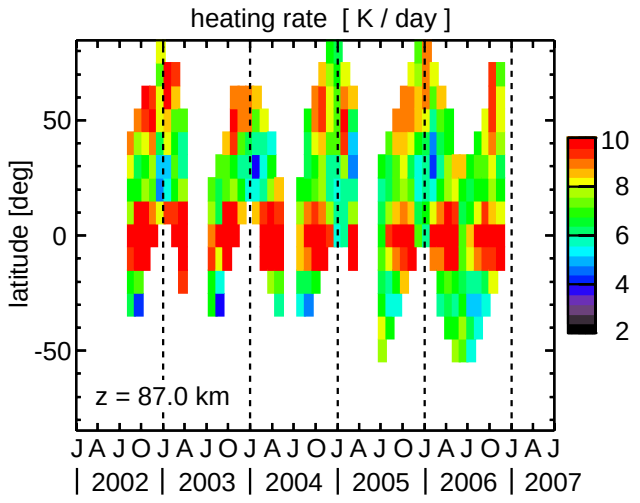

Fig. 1. Latitudinal distribution of chemical heating rates derived from SCIAMACHY hydroxyl nightglow emissions at 87 km altitude for the period 2002–2006.

based stations (e.g. Coy, 1979; Jacobi et al., 1997; Riggin et al., 1997; Namboothiri et al., 2002a,b), as well as from satellite data sets (e.g. Luo et al., 2002; Limpasuvan and Wu, 2003; Garcia et al., 2005; Riggin et al., 2006).

The observation of global scale waves from satellites has the advantage that the whole spatial structure of the wave modes can be studied. In addition, global observations can help to understand the whole global picture of wave activity and the physical processes involved. Effects of great importance for the global circulation are, for example, the modulation of gravity waves by planetary scale waves (e.g. Manson et al., 2002). Another field of interest are the interaction of longer period waves with solar tides (e.g. Palo et al., 2007; Salby and Callaghan, 2008).

One problem inherent in Earth observation from satellite platforms in low Earth orbit is the asynoptic nature of the measurement pattern. Therefore special methods have been developed to derive space-time spectra from the asynoptically sampled data (e.g. Hayashi, 1980; Salby, 1982a,b; Wu et al., 1995). In the space-time Fourier spectra the different wave modes can be identified by their characteristic frequencies and zonal wavenumbers.

With these space-time Fourier techniques frequencies of up to 1 cycle/day (periods of about 1 day or longer) can be resolved unambiguously if satellite data are available for both ascending and descending parts of the satellite orbit (Hayashi, 1980; Salby, 1982a,b; Wu et al., 1995). The situation is different if data are available only for the descending or, as is the case for the SCIAMACHY hydroxyl nightglow data, only for the ascending part of the satellite orbit. In this case only frequencies of up to 0.5 cycles/day (periods of about 2 days or longer) can be resolved unambiguously.

In our analysis we investigate the spectral signatures of planetary scale waves with periods between about 2 and 30 days in chemical heating rates derived from SCIAMACHY hydroxyl nightglow data as well as in SABER temperature data derived from 15 μm CO_2 infrared limb emissions. Aliasing effects in the SCIAMACHY spectra due to the fact that nightglow data are only available for the ascending part of the satellite orbit as well as effects due to SCIAMACHY sampling irregularities will be identified by comparison with the SABER spectra.

In Sect. 2 we describe how chemical heating rates can be derived from OH nightglow emissions. In Sect. 3 the space-time Fourier method used to derive space-time spectra for both SCIAMACHY and SABER data is briefly introduced. In Sect. 4 the resulting space-time spectra are discussed. Effects caused by differences in the SCIAMACHY and SABER sampling patterns are investigated in Sect. 5 by sampling the SABER analyses with the SCIAMACHY measurement grid. Finally, in Sect. 6 we summarize the results and draw some conclusions.

2 SCIAMACHY hydroxyl nightglow emissions and chemical heating rates

The importance of chemical heating for the energy budget of the mesopause region has been demonstrated, for example, by Brasseur and Offermann (1986). The chemical reaction of atomic hydrogen and ozone producing vibrationally excited hydroxyl

$$H + O_3 \rightarrow OH(v) + O_2 \qquad \text{(R1)}$$

is the main source of heat in the altitude region between 83 and 90 km (e.g. Mlynczak and Solomon, 1991; Riese et al., 1994). Hydroxyl vibrational modes up to v=9 are excited and the OH molecule radiates strongly through vibration-rotation transitions. In this region, the OH(v) abundance is up to 10 times higher during nighttime than during daytime. Therefore we concentrate on the nighttime measurements of hydroxyl nightglow made by SCIAMACHY.

The latitude coverage of the nighttime data is between about 50° S–20° N and 10° N–80° N depending on season and the various calibration measurements carried out during the night. More details about the SCIAMACHY observations of nighttime OH emissions can be found, for example, in von Savigny et al. (2004) and Kaufmann et al. (2008), and an instrument description can be found in Bovensmann et al. (1999).

From nighttime hydroxyl emissions chemical heating rates were derived for the H+O_3 reaction (see Kaufmann et al., 2008). Figure 1 shows the latitudinal variation of the heating rates derived for 87 km altitude for the period 2002–2006. Heating rates are maximum at the equator and have another maximum at mid latitudes. In addition, annual and semi-annual variations can be clearly identified.

This work will however focus on shorter term variability due to planetary scale waves with periods from about 2–30 days. Our analyses are based on space-time Fourier analysis (see Sect. 3). From Fig. 1 it can be seen that the latitude coverage of the SCIAMACHY data used for this analysis varies strongly during the 4–5 year period considered. This has the consequence that the space-time Fourier analysis is accomplished. Further, seasonal variations of the planetary scale wave modes will not all be fully captured because there is no continuous latitudinal coverage.

3 Analysis method: windowed space-time spectral analysis of satellite data

To derive space-time spectra from the asynoptically sampled satellite data we follow the method described in Ern et al. (2008). The data are arranged into latitude/altitude bins. For the so obtained longitude/time-series for each of the bins a two-dimensional Fourier transform can then be carried out, resulting in zonal wavenumber/frequency spectra. Since satellite data are sampled asynoptically, i.e. are not given on a regular longitude/time grid, simple two-dimensional fast Fourier transform (FFT) cannot be applied. For a more detailed discussion see Salby (1982a,b). In our approach we use a least-squares method, similar to the one by Wu et al. (1995), to derive amplitudes and phases of the independent space-time Fourier coefficients for each of the latitude/altitude bins.

In order to investigate temporal variations of the space-time spectra, we subdivide the whole data set into non-overlapping time windows and carry out a windowed space-time Fourier analysis instead of analyzing the data set as a whole. A time window length of 31 days is used, which accounts for the seasonal variations expected in the data analyzed and at the same time provides good spectral resolution of the space-time spectra. But different from Ern et al. (2008), which is focused on the analysis of equatorial wave modes, we do not calculate symmetric and antisymmetric spectra with respect to the equator for a given altitude. Instead, the spectral analyses for each latitude and altitude are used without averaging.

3.1 SABER temperatures

One part of our analysis is based on SABER version 1.06 temperature data. The SABER instrument onboard the TIMED satellite measures temperatures and several trace gases from the tropopause region to above 100 km (e.g. Mlynczak, 1997; Russell et al., 1999; Yee et al., 2003).

Space-time spectra are calculated from residual temperatures for the latitudes from 80° S to 80° N in 4° steps, according to the horizontal sampling distance of about 500 km along the satellite track. Due to the orbit geometry of the TIMED satellite zonal wavenumbers up to 6–7 and frequencies up to 1 cycle/day can be resolved by the asynoptic sampling. The SABER data used are given on fixed geometric altitudes from 15 km to above 100 km in 1-km steps. However, it should be kept in mind that the vertical resolution of the SABER instrument given by the instantaneous vertical field-of-view is about 2 km, i.e. somewhat worse.

The SABER instrument covers all local times due to the precession of the TIMED satellite orbit with a cycle period of about 60 days. Every 60 days SABER changes from a northward viewing towards a southward viewing measurement mode and vice versa. The latitudinal coverage is about 50° S–80° N in the northward viewing and about 80° S–50° N in the southward viewing measurement mode. This means that only the latitude range 50° S–50° N is covered continuously and therefore only shown in Fig. 3 in Sect. 4. Because both ascending and descending parts of the satellite orbit are available for SABER temperature data derived from the 15 μm CO_2 emission space-time spectra of residual temperatures can resolve frequencies of up to 1 cycle/day.

Because the SABER data are a very comprehensive data set SABER space-time spectra are well suited for a comparison with SCIAMACHY space-time spectra to investigate effects of the different sampling, as well as differences arising from the measurement of different limb emissions (SCIAMACHY: OH layer vs. SABER: optically thin CO_2 emissions) which could bring about different observational filters and thus different responses to atmospheric waves.

3.2 SCIAMACHY heating rates

The other part of our analysis is based on space-time spectra calculated for chemical heating rates derived from SCIAMACHY hydroxyl nightglow data using the same 31-day time windows as for SABER. Both SABER and SCIAMACHY analyses cover the same time period from August 2002 until December 2006. Due to the orbit geometry of the Envisat satellite also zonal wavenumbers up to 6–7 and frequencies up to 1 cycle/day potentially can be resolved by the asynoptic sampling. However, since nightglow data are only available for the ascending (nighttime) part of the orbit only frequencies of up to about 0.5 cycles/day can be resolved in our analysis.

The SCIAMACHY sampling pattern is not as regular as the SABER sampling pattern because the latitude band where nightglow data are available shifts with season. In addition, there are some missing data and the noise level is higher. Therefore space-time spectra are derived from residual heating rates for the latitudes from 50° S to 80° N in 10° steps. By using larger latitude intervals of 10° instead of 4° a higher number of data points enters the spectral analyses for a given latitude and the effects of increased noise and missing data are compensated to some extent.

Due to the different sampling patterns of SCIAMACHY and SABER we do not expect complete agreement between SCIAMACHY and SABER spectra. The latitude coverage

of SCIAMACHY is strongly dependent on the season (see Fig. 1) and only frequencies lower than about 0.5 cycles/day can be resolved unambiguously (see above). This means that aliasing effects from higher frequency waves will be present. In addition, spectral artifacts due to sampling irregularities will be enhanced (for example, there are data gaps due to calibration measurements during the nighttime part of the satellite orbit). Further, SCIAMACHY measurements are always at about the same local time (about 22:00 GMT during the ascending orbit parts) because the satellite platform is in a sun-synchronous orbit and therefore spectral signatures of tides will be different in SABER and SCIAMACHY spectra.

4 Spectral signatures of atmospheric wave modes in SCIAMACHY and SABER space-time spectra

To find out whether spectral signatures of the different prominent atmospheric wave modes in the mesopause region are present in both SCIAMACHY and SABER data we now compare space-time spectra averaged over the whole period from August 2002 until December 2006 at different latitudes for an altitude of 87 km. We will focus on latitudes where both SCIAMACHY and SABER have good data coverage. Results are presented in Fig. 2 for three latitudes: 0° (equatorial region), 20° N (subtropics) and 40° N (mid latitudes).

It should be noted that for SCIAMACHY not all latitude-time intervals shown in Fig. 1 are used for spectral analysis. To minimize aliasing effects due to data gaps space-time spectral analyses are carried out only for latitude-time intervals with more than 200 data points. This restriction applies for the single spectra used to calculate the average spectra shown in Fig. 2 as well as for the wave variance distributions shown in Fig. 3.

4.1 Equatorial region

Figure 2 shows average space-time spectra at the equator for both SCIAMACHY residual heating rates (a) and SABER residual temperatures (b). Positive frequencies denote eastward propagating waves whereas waves with negative frequencies travel westward.

In both SCIAMACHY and SABER spectra the strongest spectral components are at frequencies of 0 and ± 1 cycles/day. These components are due to stationary planetary waves and tides as well as their aliases, which show up periodically shifted by one zonal wavenumber and 1 cycle/day (e.g. Salby, 1982a,b). In the SCIAMACHY spectra these spectral components are even more prominent than in the SABER spectra. Because these strong spectral features also cause stronger aliasing and spectral leakage at higher zonal wavenumbers we cut the zonal wavenumber range of the SCIAMACHY spectra at zonal wavenumber 4, not to distract the reader from the spectral signatures of the other planetary scale waves which are mostly located at zonal wavenumbers ≤ 4. However, for comparison with the SABER spectral features and to identify effects of aliasing we show frequencies up to ± 1 cycle/day, although SCIAMACHY can resolve only frequencies of up to ± 0.5 cycles/day unambiguously.

Beneath the strong contributions caused by tides and stationary planetary waves we find in both SCIAMACHY and SABER spectra also strong spectral signatures for zonal wavenumber 1 at frequencies between 0.2 and 0.4 cycles/day, corresponding to periods between 2.5 and 5 days. These spectral signatures are due to equatorial Kelvin waves, which are confined to the equatorial region between about 20° S and 20° N. Kelvin waves observed in the lower stratosphere usually have longer periods of about 10 days and also higher zonal wavenumbers occur (e.g. Ern et al. (2008)). However, the spectral peak due to Kelvin waves shifts with altitude towards higher frequencies and lower zonal wavenumbers (e.g. Garcia et al., 2005) and the periods between about 2 and 5 days observed in the mesopause region are in good agreement with previous findings (e.g. Salby et al., 1984; Garcia et al., 2005).

The latitude-time distribution of wave variances due to Kelvin waves is shown in Fig. 3a for SCIAMACHY and Fig. 3b for SABER at 87 km altitude. Wave variances are obtained from the single 31-day space-time analyses by applying a band pass filter for zonal wavenumber 1 and frequencies between 0.1 and 0.4 cycles/day (periods between 2.5 and 10 days), i.e. the location of the Kelvin wave peak in the average spectra shown in Fig. 2. In both SCIAMACHY and SABER distributions we find high Kelvin wave variances only in the latitude band between about 20° S and 20° N as expected.

It should be noted that in Fig. 3 for SCIAMACHY the latitude-time coverage is somewhat worse than in Fig. 1 because only latitude-time intervals with more than 200 data points are considered (see above). In addition, for the results shown in Fig. 3 the median spectral background (determined from zonal wavenumbers >2), caused by mesoscale gravity waves not resolved by the satellite sampling, spectral artifacts, and measurement noise, is subtracted for both SCIAMACHY and SABER data to highlight the variations of the planetary scale wave modes discussed here (see also Ern et al., 2008).

4.2 Subtropics

Also shown in Fig. 2 are average space-time spectra at 20° N for SCIAMACHY (d) and SABER (e). We still find strong spectral features due to tides and stationary planetary waves. In addition, there is another strong spectral feature in the SABER spectrum at zonal wavenumbers 1–2 and frequencies of -0.5 cycles/day. Spectral amplitudes at $+0.5$ cycles/day are much weaker. This clearly indicates that at 87 km altitude on average we have dominant westward traveling zonal wavenumber 1 and 2 waves with periods of 2 days and shorter. Together with the fact that this spectral peak

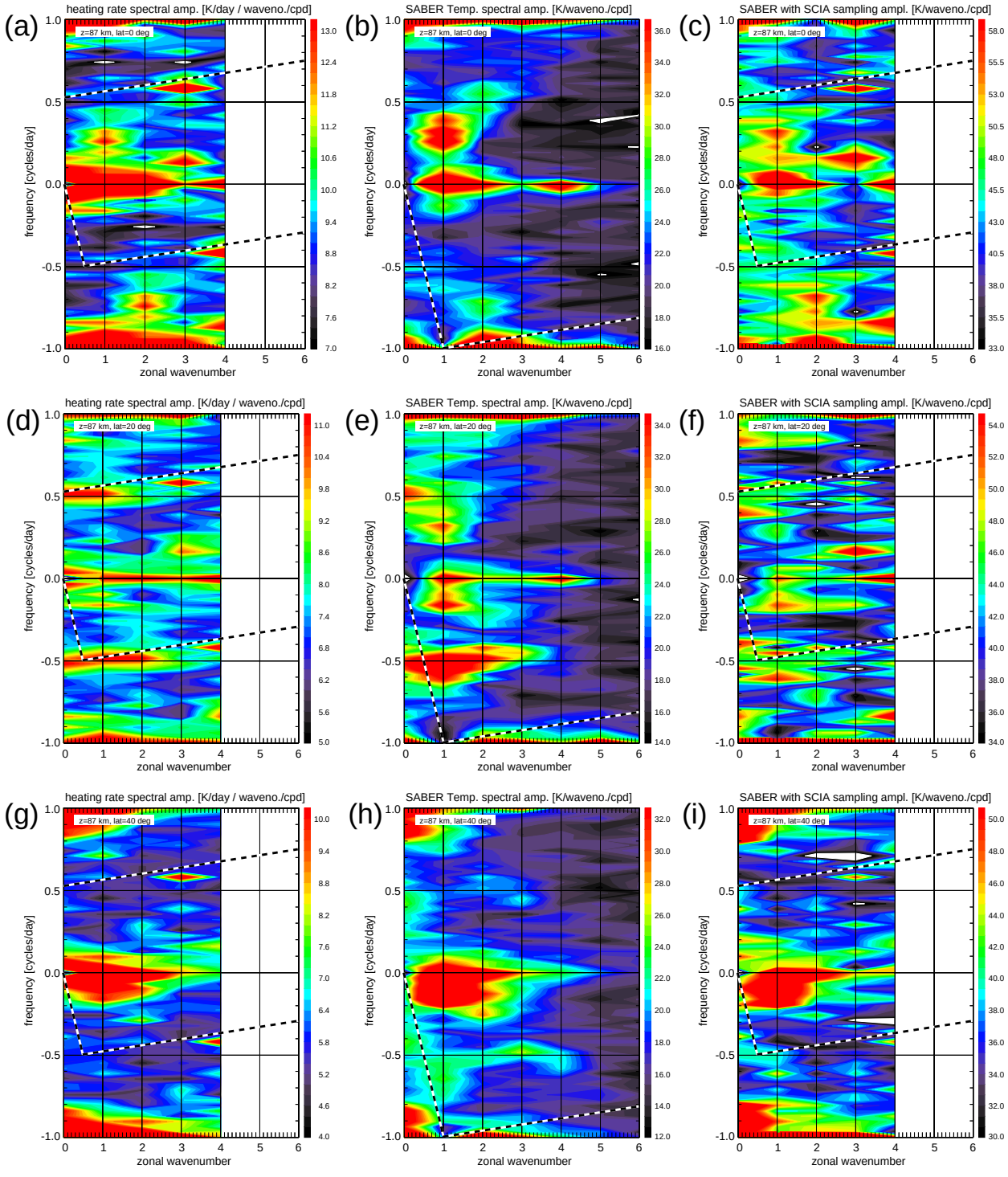

Fig. 2. Space-time spectra averaged over the period 2002–2006 of residual SCIAMACHY heating rates at 87 km altitude at the equator **(a)**, 20° N **(d)** and 40° N **(g)**. Positive frequencies denote eastward and negative frequencies westward traveling waves, respectively. For comparison also average space-time spectra of residual SABER temperatures are shown at 87 km altitude at the equator **(b)**, 20° N **(e)** and 40° N **(h)**, as well as "artificial" space-time spectra obtained by sampling the SABER analysis with SCIAMACHY measurement locations and times for the same latitudes (**c**, **f**, and **i**). The spectral range that can be resolved unambiguously by the SCIAMACHY and the SABER sampling are rectangles rotated with respect to the zonal wavenumber/frequency coordinates. The boundaries of these rectangles falling into the zonal wavenumber/frequency range shown in Fig. 2 are indicated as black and white dashed lines. Due to the single node sampling the spectral range resolved by the SCIAMACHY hydroxyl nightglow data is only half the size.

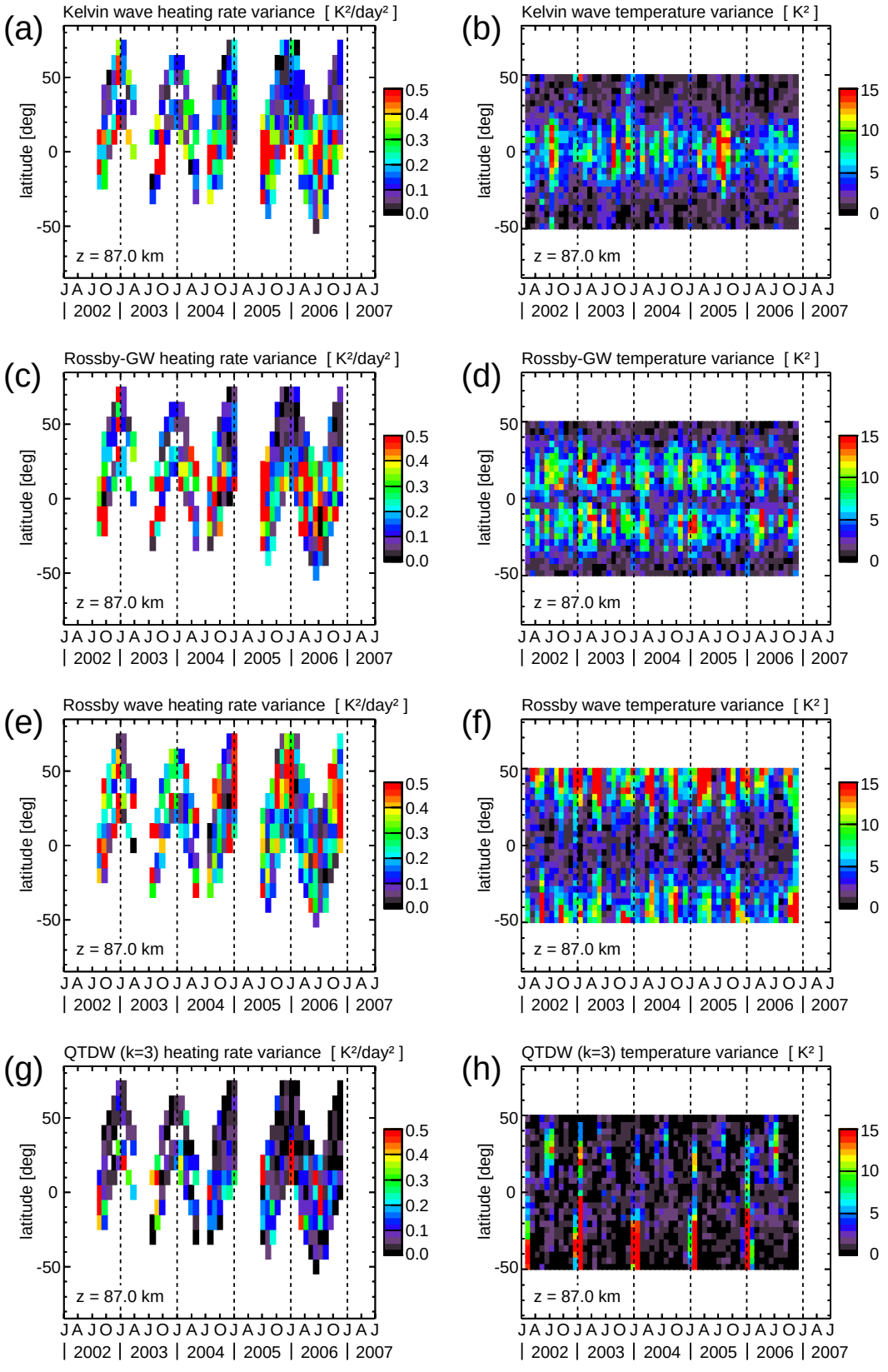

Fig. 3. Variances for different wave bands determined from SCIAMACHY (left column) and SABER (right column) space-time spectra at 87 km altitude. Shown are variances due to Kelvin waves (**a** and **b**), Rossby-gravity waves (**c** and **d**), Rossby waves (**e** and **f**), and quasi-2-day waves with zonal wavenumber 3 (**g** and **h**).

appears only in the subtropics this is an indication for equatorial Rossby-gravity waves. Rossby-gravity waves are an antisymmetric equatorial wave mode with an amplitude minimum at the equator, high amplitudes in the tropics and subtropics, and amplitudes decreasing again towards higher latitudes.

In Fig. 3d the SABER variances attributed to Rossby-gravity waves are shown using a band pass for zonal wavenumber 1 and frequencies between -0.4 and -0.7 cycles/day (periods between about 1.4 and 2.5 days), covering the bulk of the spectral feature shown in Fig. 2d and 2e. And indeed, we find the pronounced latitudinal structure with maxima at about 20° S and 20° N.

This spectral signature can also clearly be identified in the SCIAMACHY spectrum. However, since only frequencies of up to 0.5 cycles/day can be resolved unambiguously, the direction (eastward or westward) cannot clearly be determined from the SCIAMACHY spectrum alone. Like for SABER the wave variances determined from SCIAMACHY spectra (Fig. 3c) show the characteristic latitudinal structure, but the latitude-time distribution is much noisier than the SABER variances in Fig. 3d.

Again, the results are in good agreement with previous findings for equatorial Rossby-gravity waves in the mesopause region (e.g. Garcia et al., 2005). It should be noted that quasi-2-day waves, which are much more prominent in the literature, usually appear at higher latitudes and only around the summer solstices. In addition, the most prominent mode is the westward propagating zonal wavenumber 3. Therefore the observed feature is likely not a quasi-2-day wave.

In both SCIAMACHY and SABER spectra there are also indications for a westward traveling wave, having zonal wavenumber 1 and a period of between about 5 and 10 days (for discussion see Sect. 4.3). In the SABER spectrum there are still indications of Kelvin waves at wavenumber 1 and frequencies between about 0.2 and 0.5 cycles/day. This spectral feature, however, does no longer show up in the SCIAMACHY spectrum. In Sect. 5 we will investigate whether this is due to the different sampling of SABER and SCIAMACHY.

4.3 Midlatitudes

Finally, Fig. 2g and 2h shows SCIAMACHY and SABER space-time spectra at 40° N, respectively. Again, strong tidal signatures and signatures due to stationary planetary waves can be found. However, the spectral peak due to equatorial Rossby-gravity waves is no longer present in the SCIAMACHY spectrum and only weakly indicated in the SABER spectrum, and there are also no more indications of equatorial Kelvin waves.

Instead, a strong spectral peak has appeared at zonal wavenumbers 1–2 and frequencies in the range between about -0.2 and 0 cycles/day. This spectral peak can be found in both SCIAMACHY and SABER spectra. Obviously, this spectral feature is caused by westward traveling long period planetary (Rossby) waves with periods in the range of about 5–30 days. This period range is also in good agreement with the range expected from previous observations (see Sect. 1).

The wave variances due to Rossby waves are obtained by applying a band pass for zonal wavenumber 1 and frequencies between -0.25 and -0.05 cycles/day (periods between 4 and 20 days) from SCIAMACHY (Fig. 3e) and SABER (Fig. 3f) space-time spectra. From Fig. 3e and f we can see that, as expected, Rossby waves at 87 km altitude mainly appear at mid and high latitudes. Again, the SCIAMACHY latitude-time distribution is much noisier.

Another spectral feature is only visible in the SABER spectrum: There is an additional spectral peak at zonal wavenumber 3 and frequencies of about -0.5 cycles/day. This indicates that also quasi-2-day waves are present in the SABER spectra, but not in the SCIAMACHY spectra. The fact that the quasi-2-day wave signature is not present in the SCIAMACHY data can be explained by the strong seasonality of the quasi-2-day waves which occur mainly during summer solstices. During summer solstices, however, the latitude range covered by SCIAMACHY measurements is shifted strongly towards the winter hemisphere and the latitudes where quasi-2-day waves occur are not observed (see also Sect. 5).

Wave variances due to quasi-2-day waves are shown for SCIAMACHY (Fig. 3g) and SABER (Fig. 3h). A band pass filter is applied to separate spectral contributions at zonal wavenumber 3 and frequencies between -0.6 and -0.4 cycles/day (periods between about 1.7 and 2.5 days).

Very sharp pronounced peaks of wave variances due to quasi-2-day waves can be identified in the SABER quasi-2-day wave variances (Fig. 3h) especially on the Southern Hemisphere during southern summer solstices. Wave variances on the Northern Hemisphere during boreal summer solstices are also present, but much weaker. In addition, there are indications that during southern summer solstices part of the wave activity can penetrate across the equator and spreads on the Northern Hemisphere.

In the SCIAMACHY latitude-time cross section (Fig. 3g) we do not find clear signatures of wave variances due to quasi-2-day waves. One reason is that the SCIAMACHY latitudinal coverage is shifted towards the winter hemisphere during the summer solstices. Nevertheless, part of the quasi-2-day waves penetrating across the equator should be visible. However, this quasi-2-day signal is obviously too weak and is masked by spectral noise or spectral artifacts (see also Sect. 5).

5 SABER analyses sampled with SCIAMACHY measurement locations – the effect of different sampling patterns

Although in Sect. 4 good overall agreement has been found between SCIAMACHY and SABER average space-time spectra, there are still some differences that cannot be explained easily. For example, the Kelvin wave spectral signature at 20° N is present in the SABER spectrum, but not in the SCIAMACHY spectrum, or quasi-2-day waves at mid latitudes are likely not observed by SCIAMACHY. There are also some spectral features in the SCIAMACHY spectra which are not observed by SABER.

To find out whether the observed differences are mainly due to the different SCIAMACHY and SABER sampling patterns or if other reasons apply, we will now perform another analysis. We use the SABER spectral analysis to calculate values of residual temperatures at SCIAMACHY measurement locations. Then the space-time spectral analysis is carried out again for these "artificial" data at SCIAMACHY measurement locations. Differences between the SABER spectra and the SCIAMACHY spectra resulting from the "artificial" data will be mainly caused by the different sampling patterns. The remaining differences with respect to the original SCIAMACHY spectra shown in Sect. 4 will be due to other effects.

The "artificial" spectra resulting from this interpolation of SABER residual temperatures on SCIAMACHY measurement locations are shown in Fig. 2c, 2f, and 2i for the equator, 20° N, and 40° N, respectively.

First of all, the "artificial" spectra shown in Fig. 2c, 2f, and 2i have an increased spectral background with respect to the original SABER spectra shown in Fig. 2b, 2e, and 2h. This is as expected because enhanced aliasing and spectral artifacts occur since the SABER space-time analysis is sampled with only the ascending node of the SCIAMACHY measurement grid. In particular, spectral peaks at zonal wavenumber 3 and frequencies of 0.2 and 0.6 cycles/day, which occur in both the original (Fig. 2a, 2d, and 2g) and the "artificial" SCIAMACHY spectra (Fig. 2c, 2f, and 2i), but not in the original SABER spectra (Fig. 2b, 2e, and 2h), can most likely be attributed to the irregularities of the SCIAMACHY sampling pattern.

Of course, also aliases of these artifacts occur, for example, at zonal wavenumber 4 and frequencies of about -0.8 and -0.4 cycles/day in both original and "artificial" SCIAMACHY spectra. However, it should be noted that the strongest spectral artifacts in the frequency range between -0.5 and 0.5 cycles/day occur at zonal wavenumbers 3 and higher. Consequently, the spectral features of most global wave modes, which are at zonal wavenumbers 1 and 2, are only moderately affected.

By comparing "artificial" and original SCIAMACHY spectra with the original SABER spectra we find that part of the differences observed between SCIAMACHY and SABER for the wave modes discussed in Sect. 4 can, indeed, be explained by the different sampling patterns. For example, the Kelvin wave spectral feature, which is still visible in the original SABER spectra at 20° N (see Fig. 2e), is strongly suppressed in the "artificial" spectra obtained by resampling SABER with SCIAMACHY coordinates (see Fig. 2f), just like in the original SCIAMACHY spectra (Fig. 2d). In addition, the spectral peak due to quasi-2-day waves at zonal wavenumber 3 and frequency of about -0.5 cycles/day is visible only in the original SABER spectra, but not in the "artificial" spectra based on the SCIAMACHY sampling pattern (see Fig. 2f), as well as the original SCIAMACHY spectra (Fig. 2g).

This means that most of the differences found between original SCIAMACHY and SABER spectra can be explained with the different sampling patterns. It is also demonstrated that both SCIAMACHY and SABER data give a consistent picture of the global scale wave modes at the mesopause.

6 Summary and conclusions

We carried out a windowed space-time spectral analysis of chemical heating rates derived from OH nightglow emissions measured by the SCIAMACHY instrument. Since only data of the ascending orbit part is available periods of about 2 days and longer can be resolved unambiguously in the SCIAMACHY space-time spectra. There is also a strong seasonal shift of the SCIAMACHY sampling pattern and there are data gaps, for example, due to calibration measurements carried out during the nighttime part of the Envisat satellite orbit. Consequently, the SCIAMACHY space-time spectra show enhanced aliasing and some spectral artifacts caused by sampling irregularities and measurement noise.

We therefore also carried out the same space-time spectral analysis for SABER temperatures. Since SABER measurements are available for both ascending and descending orbit parts, periods of up to 1 day can be resolved by the sampling pattern. This means that the SABER spectra can be used to identify effects of aliasing in the SCIAMACHY spectra.

In both SCIAMACHY and SABER space-time spectra we find clear spectral signatures due to equatorial Kelvin and Rossby-gravity waves. In addition, at mid latitudes also spectral contributions due to Rossby waves are present in both SCIAMACHY and SABER spectra. Another spectral feature due to quasi-2-day waves at zonal wavenumber 3 and period of about 2 days is only visible in the SABER spectra.

We also derived latitude-time distributions of wave variances from the space-time spectra. In both SCIAMACHY and SABER wave variances the expected characteristic latitudinal structure of the Kelvin waves with an equatorial maximum is clearly visible. Also the Rossby-gravity waves show the expected equatorial minimum and maxima in the subtropics. In both SCIAMACHY and SABER analyses Rossby wave variances are enhanced at mid and high latitudes.

Quasi-2-day waves are visible only in the SABER wave variances and not in the SCIAMACHY longitude-time distribution. This is mainly caused by the fact that quasi-2-day wave activity has maxima always on the summer hemisphere around the summer solstices and the SCIAMACHY latitudinal coverage is shifted towards the winter hemisphere during these periods.

By sampling residual temperatures derived from the SABER space-time spectral analyses with the SCIAMACHY measurement locations and times we find that most of the differences between average SABER and SCIAMACHY space-time spectra can be explained by the different sampling patterns. In particular, the strongest spectral artifacts are located at zonal wavenumbers of 3 and higher.

Together with the fact that most wave activity in the mesopause region is at zonal wavenumbers 1 and 2 this means that, in spite of the reduced information provided by the SCIAMACHY spectra as a result of the reduced sampling, the spectral contributions of most of the wave modes present in the mesopause region are only moderately affected by spectral artifacts and valuable information can be obtained from the SCIAMACHY spectra. Our analysis shows that both SCIAMACHY and SABER data sets give a consistent picture of the wave modes in the mesopause region. Because the SCIAMACHY measurement grid is more regular since mid 2005 even better results can be expected in future when further years of data will be available for spectral analysis.

Acknowledgements. This study has been partly supported by Deutsche Forschungsgemeinschaft (DFG) under Grant RI 1546/1-2 (HYDOX) within the DFG priority program CAWSES (SPP 1176). We thank ESA for providing the SCIAMACHY data within the Cat-1 project 2515. We also like to thank the team at the Institute of Environmental Physics, University of Bremen for helpful discussions.

Topical Editor K. Kauristie thanks C. Jacobi and another anonymous referee for their help in evaluating this paper.

References

Bovensmann, H., Burrows, J. P., Buchwitz, M., Frerick, J., Noël, S., and Rozanov, V. V.: SCIAMACHY: Mission objectives and measurement modes, J. Atmos. Sci., 56, 127–150, 1999.

Brasseur, G. and Offermann, D.: Recombination of atomic oxygen near the mesopause – interpretation of rocket data, J. Geophys. Res., 91, 818–824, 1986.

Coy, L.: A possible 2-day oscillation near the tropical stratopause, J. Atmos. Sci., 36, 1615–1618, 1979.

Ern, M., Preusse, P., Krebsbach, M., Mlynczak, M. G., and Russell III, J. M.: Equatorial wave analysis from SABER and ECMWF temperatures, Atmos. Chem. Phys., 8, 845–869, 2008, http://www.atmos-chem-phys.net/8/845/2008/.

Garcia, R. R., Lieberman, R., Russell III, J. M., and Mlynczak, M. G.: Large-scale waves in the mesosphere and lower thermosphere observed by SABER, J. Atmos. Sci., 62, 4384–4399, 2005.

Hayashi, Y.: A method of estimating space-time spectra from polar-orbiting satellite data, J. Atmos. Sci., 37, 1385–1392, 1980.

Jacobi, Ch., Schminder, R., and Kürschner, D.: The quasi 2-day wave as seen from D1 LF wind measurements over Central Europe (52° N, 15° E) at Collm, J. Atmos. Solar-Terr. Phys., 59, 1277–1286, 1997.

Kaufmann, M., Lehmann, C., Hoffmann, L., Funke, B., López-Puertas, M., von Savigny, C., and Riese, M.: Chemical heating rates derived from SCIAMACHY vibrationally excited OH limb emission spectra, Adv. Space Res., 41, 1914–1920, doi:10.1016/j.asr.2007.07.045, 2008.

Limpasuvan, V. and Wu, D. L.: Two-day wave observations of UARS Microwave Limb Sounder mesospheric water vapor and temperature, J. Geophys. Res., 108, 4307, doi:10.1029/2002JD002903, 2003.

Luo, Y., Manson, A. H., Meek, C. E., Meyer, C. K., Burrage, M. D., Fritts, D. C., Hall, C. M., Hocking, W. K., MacDougall, J., Riggin, D. M., and Vincent, R. A.: The 16-day planetary waves: multi-MF radar observations from the arctic to equator and comparisons with the HRDI measurements and the GSWM modelling results, Ann. Geophys., 20, 691–709, 2002, http://www.ann-geophys.net/20/691/2002/.

Manson, A. H., Meek, C. E., Luo, Y., Hocking, W. K., MacDougall, J., Riggin, D., Fritts, D. C., and Vincent, R. A.: Modulation of gravity waves by planetary waves (2 and 16 d): observations with the North American-Pacific MLT-MFR radar network, J. Atmos. Solar-Terr. Phys., 65, 85–104, 2002.

Mlynczak, M. G. and Solomon, S.: Middle atmosphere heating by exothermic chemical reactions involving odd-hydrogen species, Geophys. Res. Lett., 18, 37–40, 1991.

Mlynczak, M. G.: Energetics of the mesosphere and lower thermosphere and the SABER instrument, Adv. Space Res., 44, 1177–1183, 1997.

Namboothiri, S. P., Kishore, P., and Igarashi, K.: Climatological studies of the quasi 16-day oscillations in the mesosphere and lower thermosphere at Yamagawa (31.2° N, 130.6° E), Japan, Ann. Geophys., 20, 1239–1246, 2002a, http://www.ann-geophys.net/20/1239/2002/.

Namboothiri, S. P., Kishore, P., and Igarashi, K.: Observations of the quasi-2-day wave in the mesosphere and lower thermosphere over Yamagawa and Wakkanai, J. Geophys. Res., 107, 4320, doi:10.1029/2001JD000539, 2002b.

Palo, S. E., Roble, R. G., and Hagan, M. E.: Middle atmosphere effects of the quasi-two-day wave determined from a General Circulation Model, Earth Planets Space, 51, 629–647, 1999.

Palo, S. E., Forbes, J. M., Zhang, X., Russell III, J. M., and Mlynczak, M. G.: An eastward propagating two-day wave: Evidence for nonlinear planetary wave and tidal coupling in the mesosphere and lower thermosphere, Geophys. Res. Lett., 34, L07807, doi:10.1029/2006GL027728, 2007.

Riese, M., Offermann, D., and Brasseur, G.: Energy released by recombination of atomic oxygen and related species at mesopause heights, J. Geophys. Res., 99, 14585–14593, 1994.

Riggin, D. M., Fritts, D. C., Tsuda, T., and Nakamura, T.: Radar observations of a 3-day Kelvin wave in the equatorial mesosphere, J. Geophys. Res., 102, 26141–26157, 1997.

Riggin, D. M., Liu, H.-L., Lieberman, R. S., Roble, R. G., Russell III, J. M., Mertens, C. J., Mlynczak, M. G., Pancheva, D., Franke, S. J., Murayama, Y., Manson, A. H., Meek, C. E., and Vincent, R. A.: Observations of the 5-day wave in the mesosphere and lower thermosphere, J. Atmos. Solar-Terr. Phys., 68, 323–339,

2006.

Russell III, J. M., Mlynczak, M. G., Gordley, L. L., Tansock, J., and Esplin, R.: An overview of the SABER experiment and preliminary calibration results, Proceedings of SPIE, 3756, 277–288, 1999.

Salby, M. L.: Sampling theory for asynoptic satellite observations, Part I: Space-time spectra, resolution, and aliasing, J. Atmos. Sci., 39, 2577–2600, 1982.

Salby, M. L.: Sampling theory for asynoptic satellite observations, Part II: Fast Fourier synoptic mapping, J. Atmos. Sci., 39, 2601–2614, 1982.

Salby, M. L.: Survey of planetary-scale traveling waves: The state of theory and observations, Rev. Geophys. Space Phys., 22, 209–236, 1984.

Salby, M. L., Hartmann, D. L., Bailey, P. L., and Gille, J. C.: Evidence for equatorial Kelvin modes in Nimbus–7 LIMS, J. Atmos. Sci., 41, 220–235, 1984.

Salby, M. L. and Callaghan, P. F.: Interaction of the 2-day wave with solar tides, J. Geophys. Res., 113, D14121, doi:10.1029/2006JD007892, 2008.

von Savigny, C., Eichmann, K.-U., Llewellyn, E. J., Bovensmann, H., Burrows, J. P., Bittner, M., Höppner, K., Offermann, D., Taylor, M. J., Zhao, Y., Steinbrecht, W., and Winkler, P.: First near-global retrievals of OH rotational temperatures from satellite-based Meinel band emission measurements, Geophys. Res. Lett., 31, L15111, doi:10.1029/2004GL020410, 2004.

Wu, D. L., Hays, P. B., and Skinner, W. R.: A least squares method for spectral analysis of space–time series, J. Atmos. Sci., 52, 3501–3511, 1995.

Yee, J. H., Talaat, E. R., Christensen, A. B., Killeen, T. L., Russell, J. M., and Woods, T. N.: TIMED instruments, Johns Hopkins APL Technical Digest, 24, 156–164, 2003.